Top Catal (2011) 54:881–887
DOI 10.1007/s11244-011-9696-8

ORIGINAL PAPER

Selective Conversion of Ethane to Ethene via Oxidative Dehydrogenation Over Ca-doped ThO_2 Using CO_2 as Oxidant

Tinku Baidya · Niels van Vegten · Alfons Baiker

Published online: 6 August 2011

Abstract Ca-doped ThO_2, synthesized by solution combustion method was tested for dehydrogenation of ethane with CO_2. Doping ThO_2 with Ca resulted in the creation of oxide ion vacancies and an increased conversion of ethane compared to pure ThO_2. On $Th_{0.75}Ca_{0.25}O_2$ selectivity to ethene was 97 at 46% ethane conversion at 725 °C. Well-known reference catalysts like 5%Cr/TS-1 or OMS-2 showed significantly lower selectivity, but the former was more active under the same conditions.

Keywords Oxidative dehydrogenation · Ethane · Ethene · CO_2 · Solid solution · Thorium oxide · Ca doping

1 Introduction

Ethane is the second major component of natural gas, which makes it a potential source of chemicals such as light olefins, oxygenates and aromatic hydrocarbons [1]. Converting the abundant ethane to ethylene at low temperature has been a challenge in chemical and petrochemical industry for many years [2].

Oxidative dehydrogenation (ODH) is the simplest process of partial oxidation of light alkanes. A number of catalysts, mainly vanadium, molybdenum and other group V-based oxides have been studied as active catalyst in presence of O_2 as oxidant [3–8]. Mechanistic findings showed that V–O–S or Mo–O–S type of bridging bonds were responsible for the dehydrogenation [9, 10]. These catalysts are not as active as would be required for use in large scale production. Since oxygen is a strong oxidant, high temperature cannot be used because selectivity decreases dramatically [11].

The use of N_2O as alternative oxidation agent is troubled by the fact that selectivity can be deteriorated at higher conversion due to the formation of reactive $O^{\cdot -}$ radical species from N_2O [12, 13]. Furthermore, N_2O also faces the drawback of limited availability for any mass production of ethene. Recently, attempts have been made to utilize less reactive carbon dioxide as an oxidant for dehydrogenation of ethane to yield ethene [14, 15]. The advantage of utilization of the green house gas CO_2 as oxidant is that it might lead to higher selectivity at elevated temperatures because it is less prone to supply oxygen species for reaction. Furthermore, syngas can be obtained as a by-product of this process [16]. The main problem encountered in this reaction is catalyst deactivation due to carbon deposition and thus termination of syngas production. Up to date, Mo_2C/SiO_2 [17], Cr/H-ZSM-5 [18, 19], Cr/TS-1[20], Cr/SiO_2 [15], Ga/TiO_2 [21], and CeO_2-based oxides [22] have been used in the dehydrogenation of ethane with CO_2 as an oxidant. Among these catalysts, chromium-based catalysts have proven to be the most active for this reaction. Chromium based catalysts supported on TS-1 or Cr/H-ZSM-5 show best performance, but their reaction temperature is limited to about 650 °C, since at higher temperatures selectivity decreases significantly [20].

To our knowledge application of non-redox oxide materials for this reaction with CO_2 has not been reported in the literature, probably because of their low propensity for dissociating CO_2. We have observed in an earlier study that Ca-doped ThO_2 is capable of producing oxygen radicals [23], probably by virtue of p-type conductivity. These

T. Baidya · N. van Vegten · A. Baiker (✉)
Institute for Chemical and Bioengineering, Department of Chemistry and Applied Biosciences, ETH Zurich, 8093 Hönggerberg, HCI, Zürich, Switzerland
e-mail: baiker@chem.ethz.ch

radicals could be beneficial for partial oxidation of ethane. A mild oxidizing compound such as CO_2 could also dissociate at these oxide ion vacancy sites, producing oxide ion radicals at elevated temperature. Thus, these materials may afford a more selective process than the strong oxidant Cr(VI). With this in mind, we have explored Ca-doped ThO_2 as a catalyst for the oxidative dehydrogenation of ethane with CO_2.

2 Experimental

2.1 Catalyst Preparation

The ThO_2-based catalysts were prepared using a single step solution combustion method [24]. Stoichiometric amounts of $Th(NO_3)_4$ (Aldrich-Fine Chemicals, 99%), $Ca(NO_3)_2$ $4H_2O$ (Acros Organics, 99+ %) and tartaric acid were taken in a 300 mL crystallizing dish with water. Initially, the mixture was heated to make a transparent solution and then kept in the furnace at 500 °C. After dehydration, ignition started and within a minute the oxide product was obtained. Subsequently, the samples were calcined at 800 °C for 10 h to remove carbonaceous products.

Reference catalyst OMS-2 (octahedral molecular sieve) was prepared following the procedure described in the literature [25]. $MnCl_2{\cdot}4H_2O$ (7.5 g) was dissolved in water (50 mL). Air was bubbled into the Mn^{2+} solution at a high flow rate. Then, an aqueous solution (80 mL) containing NaOH (20 g) was added dropwise to the solution for 30 min. After 6 h, a brown colored product was obtained which was filtered, washed, and transferred into a 1 M aqueous solution of KCl (250 mL) and stirred for 12 h at room temperature for ion exchange. The product was then filtered and washed with deionized water. The K-birnessite was dried in air at 80 °C for 4 h and then placed in a furnace to calcine stepwise in air at 200, 400, 600, and 800 °C for about 2 h at each temperature.

To prepare 5%Cr/TS-1, TS-1 was synthesized following the procedure reported in the literature [26]. Two grams of Tween 20 (SIAL) were dissolved in 32 g of distilled water. This surfactant solution was added to 19.2 g of tetrapropylammonium hydroxide (TPAOH, 25% aqueous solution, Acros Organics) under mild stirring, which resulted in a clear transparent solution. To the above micellar solution, 36 g of tetraethyl orthosilicate (Aldrich) was added dropwise under vigorous stirring which was continued for another 1 h. To this solution, 1.808 g of tetra *n*-butyl titanate (Acros Organics) in 9.12 g of isopropyl alcohol (IPA) was then added dropwise under vigorous stirring for another 1 h. Subsequently, the mixture was crystallized at 160 °C for 18 h in an autoclave. The product was recovered by centrifugation, washed with distilled water and dried (110 °C, 12 h). Then, it was heated to 800 °C by stepwise increase at an interval of 200 °C. Finally, the TS-1 was suspended in 50 cc water solution of $(NH_4)_2CrO_4$ under continuous stirring and heated until total evaporation. The resulting material was calcinated at 600 °C for 6 h.

2.2 Catalysts Characterization

X-ray diffractograms were recorded on a PANalytical X'Pert using Cu Kα ($\lambda = 1.541$ Å) radiation in step mode between 10 and 70° 2θ with a step-size of 0.017 and 0.3 s/step. Metallic Cu was used as an internal standard.

The Raman spectra of the ThO_2 based oxides were recorded in the 180° backscattering geometry, using a 532 nm excitation from a diode pumped frequency doubled Nd:YAG solid state laser (model GDLM-5015 L, Photop Suwtech Inc., China) and a custom-built Raman spectrometer equipped with a SPEX TRIAX 550 monochromator and a liquid nitrogen cooled charge-coupled device (CCD; Spectrum One with CCD 3000 controller, ISA Jobin Yovn). Laser power at the sample was $\sim$8 mW, and a typical spectral acquisition time was 1 min. The spectral resolution chosen was 2 cm^{-1}.

2.3 Catalytic Tests

The reactor set-up was a conventional gas flow system where ethane and carbon dioxide were co-fed over the catalyst. The catalyst was placed in a quartz U-tube reactor (ID 4.5 mm) which itself was placed inside a temperature controlled furnace. Typically, 400 mg of catalyst was diluted with 1000 mg of SiO_2 (white sand, Acros Organics) and kept in place between two quartz wool plugs. The quartz wool before the bed acted as a pre-heating zone. Gas flows were regulated by mass flow controllers (Brooks Instrument B. V, model 5850E). The total flow was kept at 50 cc min^{-1}, yielding a space velocity of 7500 cc $g_{cat}{}^{-1}$ h^{-1}. The temperature was measured by a thermocouple well on the outer surface of the quartz reactor at the middle of the catalyst bed. Comparative tests were performed at 725 °C. The exhaust gas was analyzed using an on-line gas chromatograph with both TCD and FID detectors, which was connected to the reactor with heated stainless steel lines. The GC (Agilent Technologies, model 6890N) was equipped with a CarbonPLOT capillary column which allowed full separation of exhaust gas components such as CO, CO_2, CH_4, C_2H_4 and C_2H_6. Each of the products was calibrated against a calibration gas mixture. Note that in some experiments small amounts (1–2%) of C_3H_6 and C_3H_8 were also observed over the Ca doped ThO_2 samples. The carbon balance was 95% on an average in all experimental runs.

Ethane conversion ($X_{C_2H_6}$) and selectivity to ethene ($S_{C_2H_4}$) are defined as:

$X_{C_2H_6}$ (%) = (moles of C_2H_6 converted × 100)/(moles of C_2H_6 in feed).
$S_{C_2H_4}$ (%) = (moles of C_2H_4 in outlet gas × 100)/(moles of C_2H_6 in feed).

CO_2 conversion (X_{CO2}) and selectivity to CO (S_{CO}) are defined as:
X_{CO_2} (%) = (moles of CO_2 converted × 100)/(moles of CO_2 in feed).
S_{CO} (%) = (moles of CO in outlet gas × 100)/(moles of CO_2 in feed).

3 Results and Discussion

3.1 Structural Characterization

The top panel in Fig. 1 presents the XRD patterns of the ThO_2 based catalysts. The XRD analysis shows that the ThO_2-based materials crystallized in the fluorite phase. From the line broadening by applying the Scherrer formula, the crystallite sizes were calculated to be 15, 8 and 7 nm for ThO_2, $Th_{0.8}Ca_{0.2}O_2$ and $Th_{0.75}Ca_{0.25}O_2$, respectively. To check the shift in peak position due to Ca substitution in ThO_2, X-ray diffraction was performed with a Cu internal standard allowing accurate determination of the position of the Cu (111) reflection at 43.32 2θ (JCPDS 4-0836). Its shift toward lower 2θ values confirms the incorporation of larger Ca^{2+} ions in the ThO_2 lattice (Fig. 1, bottom). According to Vegard's law of solid solutions, the lattice parameter changes depending on the size of the dopant ion. Thus, the shift could be attributed to the difference in ionic radii of the Ca^{2+} (8 CN 1.12 Å) ion compared to Th^{4+} (8 CN 1.05 Å). The larger the difference in ionic radii, the larger the shift of the (111) position will be. Since apparently Ca is incorporated in the ThO_2, the catalysts can be represented as $Th_{1-x}Ca_xO_2$.

Figure 2 shows the XRD patterns of the reference catalysts. OMS-2 (octahedral molecular sieve) shows the byxbyite structure (Mn_2O_3, JCPDS 41-1442, Space group: Ia-3). The reflections from chromium supported on SiO_2 and TS-1 samples correspond to the presence of Cr_2O_3 in eskolaite phase (JCPDS 1-072-4555, Space group: R-3c). The sample color was green, which also confirmed the presence of Cr_2O_3.

Figure 3a–e shows the Raman spectra of ThO_2 and Ca-doped ThO_2 samples along with pure $CaCO_3$ and a mixture of ThO_2 and $CaCO_3$. Raman spectra could give an indication of changes in the lattice due to Ca ion substitution in ThO_2. The characteristic F_{2g} symmetry peak at 465 cm^{-1}

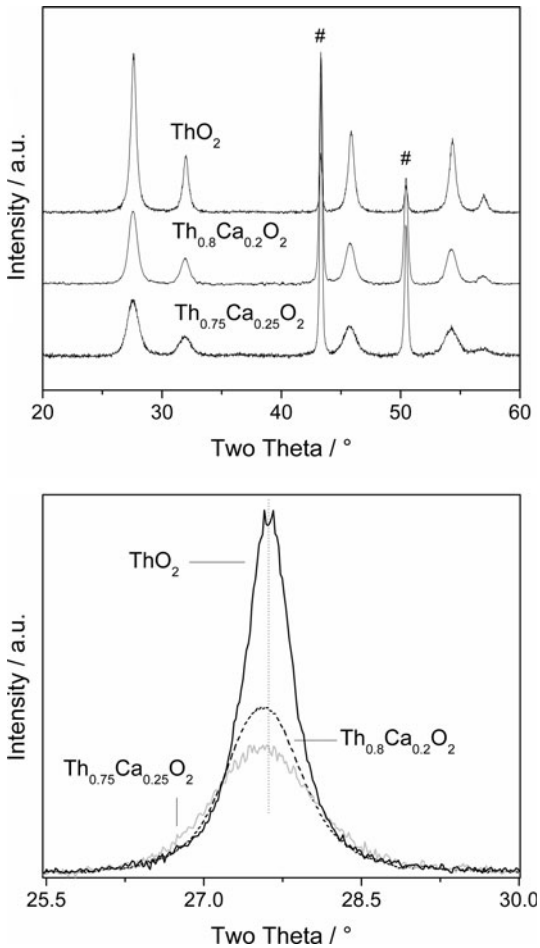

Fig. 1 XRD analysis of ThO_2, $Th_{0.8}Ca_{0.2}O_2$ and $Th_{0.75}Ca_{0.25}O_2$ (*top*), and magnified section of the XRD pattern of the (111) reflection of ThO_2, $Th_{0.8}Ca_{0.2}O_2$ and $Th_{0.75}Ca_{0.25}O_2$ (*bottom*). # Indicates the position of the reflections of the Cu standard used for these measurements

of ThO_2 is prominent. In $Th_{0.8}Ca_{0.2}O_2$ and $Th_{0.75}Ca_{0.25}O_2$, significant peak shift was not observed as ionic radii of Ca and Th ion are almost similar. This type of feature was not observed in $CaCO_3$ as well as in the mixture of ThO_2 and $CaCO_3$ (Fig. 3b, c). A similar feature was observed for CeO_2, another fluorite structure, substituted with lower valent rare earth metal ions, as reported by McBride et al. [27] and confirmed by several other groups [28–30]. They reported incorporation of various rare earth elements (RE) in CeO_2 forming $Ce_{1-x}RE_xO_{2-\delta}$ solid solutions in fluorite structure and assigned the Raman band at ~570 cm^{-1} to formation of oxide ion vacancies. This type of feature was not observed in $CaCO_3$. The appearance of such a feature in the Ca-doped ThO_2 catalysts might therefore be an indication of the presence of similar vacancies in the current systems. To confirm Ca substitution further, pure $CaCO_3$ was also analyzed. Three characteristic vibration modes, symmetric stretching (1084 cm^{-1}), in-plane

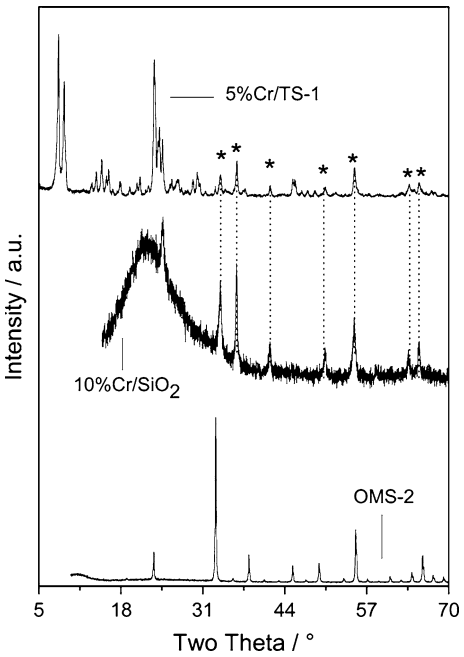

Fig. 2 XRD profiles of reference catalysts OMS-2 (Mn_2O_3, octahedral molecular sieve), 10%Cr/SiO_2 and 5%Cr/TS-1 * Indicates reflections from Cr_2O_3

bending (712 cm^{-1}) and lattice mode vibration (282 cm^{-1}) are observed in $CaCO_3$ [31]. These peaks are also observed in $CaCO_3$ and ThO_2 mixture. Interestingly, the peaks at 282 cm^{-1} and 712 cm^{-1} are missing in the Ca doped samples indicating absence of bulk $CaCO_3$. Moreover, symmetric stretching peak is lowered from 1084 to 1072 cm^{-1} and it becomes broad, which essentially means the loss of symmetry occurring due to the presence on surface. Therefore, Ca could be substituted in ThO_2 matrix and they must be containing surface carbonate species due to basic in nature.

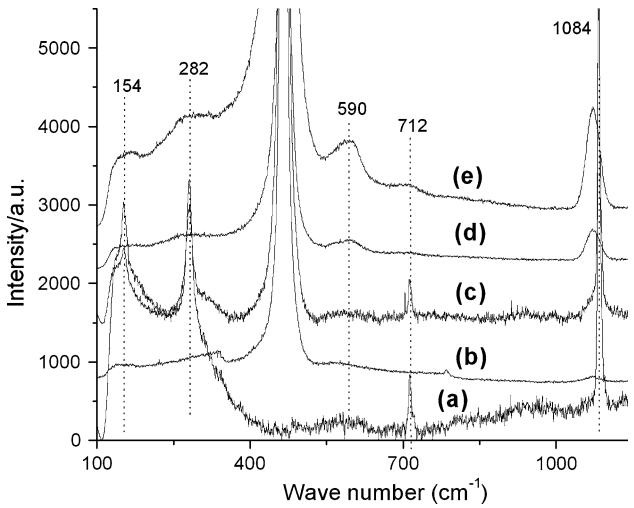

Fig. 3 Raman spectra of **a** $CaCO_3$ **b** ThO_2 **c** $ThO_2 + CaCO_3$ **d** $Th_{0.8}Ca_{0.2}O_2$ and **e** $Th_{0.75}Ca_{0.25}O_2$

3.2 Catalytic Activity

The catalytic activity of the Ca-doped ThO_2 catalyst was tested in the temperature range 600–750 °C (Fig. 4) and varying C_2H_6/CO_2 ratios (Fig. 5). Comparative data of the catalytic performances of the Ca-doped ThO_2 catalysts and the reference catalysts at a suitable reaction temperature of 725 °C are given Table 1. In Fig. 4 the temperature dependencies of conversion and selectivity to ethane of $Th_{0.75}Ca_{0.25}O_2$ catalysts are compared to those of the most active reference catalyst 5%Cr/TS-1.

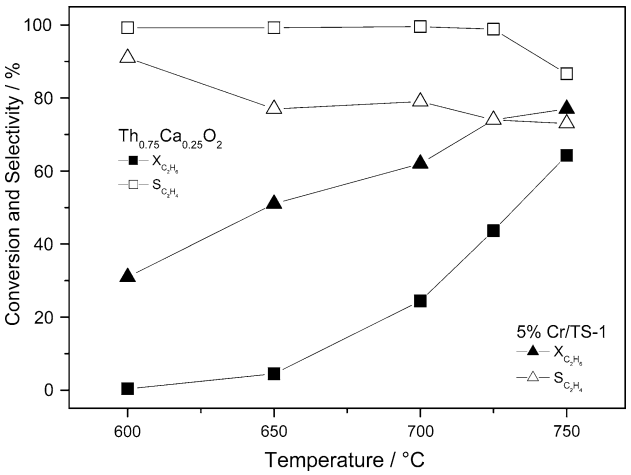

Fig. 4 Temperature dependence of conversion of ethane and selectivity to ethene over $Th_{0.75}Ca_{0.25}O_2$ and 5%Cr/TS-1 (reference catalyst). Conditions: C_2H_6:CO_2:Ar = 45:35:20%; Total flow—50 cc/min, temperature—725 °C; catalyst—0.4 and 1 g SiO_2)

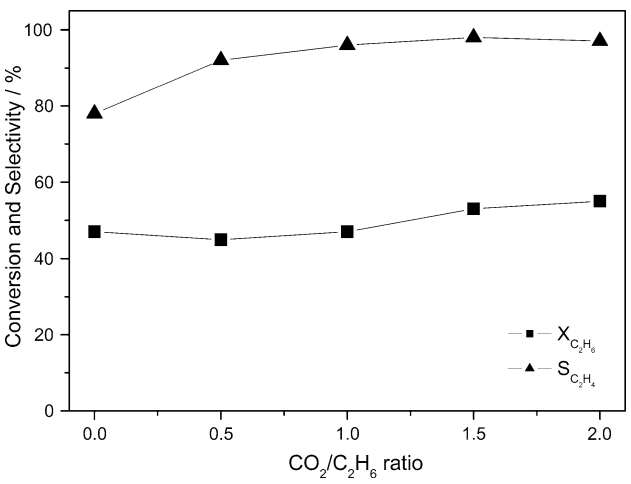

Fig. 5 Dependence of ethane conversion and selectivity to ethane on CO_2/C_2H_6 ratio over $Th_{0.75}Ca_{0.25}O_2$. Conditions: Total flow—50 cc/min, temperature—725 °C; catalyst—0.4 and 1 g SiO_2)

Table 1 Results of oxidative dehydrogenation of ethane over ThO_2 based catalysts along with reference catalysts

Entry	Catalyst	$X_{C_2H_6}$ (%)	$S_{C_2H_4}$(%)	X_{CO_2} (%)	S_{CO} (%)	Yield (%)
1	No catalyst	39	83	–[a]	–	32
2	ThO_2	17	>99	19	95	17
3	$Th_{0.75}Ca_{0.25}O_2$	46	97	43	80	45
4	$Th_{0.75}Ca_{0.25}O_2$[b]	48	78	–	–	37
5	OMS-2	38	82	–	–	31
6	5%Cr/TS-1	74	74	40	>100[c]	55
7	10%Cr/SiO_2	31	86	–	–	27

Conditions: C_2H_6:CO_2:Ar = 45:35:20% for a total flow of 50 cc min^{-1} at 725 °C. A catalyst weight of 0.4 g was used along with 1 g of SiO_2 as diluent

[a] No conversion detected

[b] C_2H_6:Ar:He = 40:20:40 (absence of CO_2)

[c] Note that selectivity to CO > 100% is probably due to some deep oxidation of hydrocarbons (ethane, ethene)

As emerges from Fig. 4, ethane conversion over 5%Cr/TS-1 was already over 30% at 600 °C, while the $Th_{0.75}Ca_{0.25}O_2$ did not show any appreciable activity at this temperature. However, over Ca/ThO_2 the conversion increased more strongly at higher temperatures reaching over 60% at 750 °C. Selectivity to ethene was much higher over $Th_{0.75}Ca_{0.25}O_2$ being >97% in the whole temperature range up to 725 °C, while over the 5%Cr/TS-1 reference catalyst it decreased from 92% at 600 °C to 74% at 725 °C. This behavior could indicate a different reaction mechanism on these catalysts. The role of Cr as active species has been elucidated in the literature [19]. Ethene formation was shown to occur by reduction of Cr(VI) species and CO_2 dissociates to re-oxidise Cr(III) to Cr(VI) under the reaction conditions. Thus, dissociated oxygen is presumably more available over this catalyst compared to the Ca/ThO_2 leading to lower selectivity at higher temperature. $Th_{0.75}Ca_{0.25}O_2$ cannot produce any oxidizing species like $Cr^{VI} = O$. Compelling evidence for a different mechanism over $Th_{0.75}Ca_{0.25}O_2$ will be presented below.

The role of CO_2 is to generate oxygen species that take part in the formation of ethene as well as to suppress carbon deposition. The dependence of ethane conversion and selectivity to ethene on the ratio CO_2/C_2H_6 is shown in Fig. 5. It shows that in the absence of CO_2 the selectivity was 78% and it increased to >97% with increasing CO_2/C_2H_6 ratio up to 1.5. Further increase in CO_2 did not show significant effect.

Table 1 shows the catalytic results over the ThO_2-based catalysts along with the three reference catalysts OMS-2, 5%Cr/TS-1, and 10%Cr/SiO_2. Note that at high temperature, thermal dehydrogenation as well as catalytic surface reaction contribute to the conversion of ethane. Significant thermal dehydrogenation of ethane occured above 700 °C which generally lead to lower selectivity. This is confirmed by the experiment without catalyst (entry 1), where 39% conversion at 83% selectivity to ethane was reached, without any detectable conversion of CO_2. An optimum temperature of 725 °C was selected for this comparative study to keep high selectivity to ethene at significant conversion of ethane. The selectivity was improved by using ThO_2-based catalysts (entry 2). Surprisingly, conversion of ethane decreased to 17% over pure ThO_2, but selectivity increased to more than 99%. 19% CO_2 was converted to CO with a selectivity of about 95%. The higher conversion was regained by Ca incorporation up to 20–25 at.% into ThO_2 (entries 3–5). In absence of CO_2 (entry 4), the conversion increased to 48% but selectivity went down to 78%. In presence of CO_2 (entry 3), conversion of ethane remained at about 46% and selectivity was maintained at about 97% over $Th_{0.75}Ca_{0.25}O_2$. The conversion of CO_2 was more than 40% and CO, H_2O and H_2 were obtained as by-product. Selectivity to CO was found to be about 80%.

Several reference catalysts OMS-2, 5%Cr/TS-1, and 10%Cr/SiO_2 were studied for comparison showing conversions of 38, 74 and 31%, and selectivities of 82, 74 and 86%, respectively. Note that the most active catalyst, 5%Cr/TS-1, had significantly lower selectivity than $Th_{0.75}Ca_{0.25}O_2$. It is an often made observation in oxidation catalysis that the more active a catalyst, the less selective it is and vice versa. Interestingly, OMS-2 seems to be poorly active as catalyst because conversion and selectivity remained almost similar to that obtained without catalysts (compare entries 1 and 6). Only 13% conversion of CO_2 was observed initially and it decreased to zero within 1 h without significant change in ethane conversion. This indicates that ethene formation over OMS-2 occurred mainly due to thermal dehydrogenation. Similarly, 10%Cr/SiO_2 showed very low conversion of CO_2 within few hours. However, 5%Cr/TS-1 showed a consistent conversion of CO_2. Interestingly, selectivity to CO significantly exceeded 100%. This could happen probably due to some

deep oxidation of hydrocarbons (ethane, ethene) to CO resulting in an apparent selectivity to CO higher than 100%.

At the temperatures employed in this study, ethane could crack under formation of carbonaceous residues on the catalyst surface [32]. Since this coking would negatively influence the catalyst performance, the long term behavior of $Th_{0.8}Ca_{0.2}O_2$ was tested. A CO_2/C_2H_6 ratio of 1.3 was used for this experiment, instead of the 0.78 in the rest of the studies. Visual inspection showed the catalyst color to have changed from white to black, indicating some deposition of carbonaceous residues. However, as Fig. 6 reveals, within the 25 h on stream, no significant changes in catalyst performance were observed. This testifies of a strong stability of the catalyst under reaction conditions, in spite of the color change observed.

Finally, it is interesting to speculate about the mechanism of the oxidative dehydrogenation process, albeit the elucidation of the mechanism was not in the focus of this work. Nevertheless the observed catalytic behavior allows some speculation. We have observed that dehydrogenation of ethane occurs in absence of catalyst at 725 °C reaching a selectivity of about 83%. On the other hand, the reaction in the presence of $Th_{1-x}Ca_xO_2$ afforded a selectivity of 97%, although conversion remained almost unchanged in both cases.

Preliminary EPR measurements on the $Th_{0.75}Ca_{0.25}O_2$ sample showed the genesis of paramagnetic oxygen species in the range of 3200–3600 Gauss after exposure to CO_2 at 725 °C. These species could be removed after subsequent exposure to ethane. The loss of paramagnetic species due to ethane exposure hints towards a surface-bound radical oxygen species. In earlier work [32], it was found that

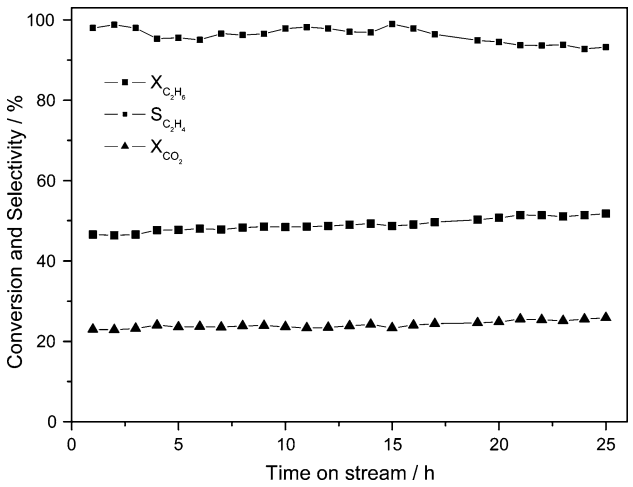

Fig. 6 Long term behavior of catalyst $Th_{0.8}Ca_{0.2}O_2$. Ethane conversion and selectivity to ethene vs. time on-stream. Conditions: C_2H_6:CO_2:Ar = 35:45:20%; total flow—50 cc/min, temperature—725 °C, catalyst—0.4 and 1 g SiO_2)

species were produced from O_2 and were stabilized in oxide ion vacancies available in $Th_{0.8}Ca_{0.2}O_2$. Possibly, disproportionation of CO_2 on the $Th_{0.75}Ca_{0.25}O_2$ catalyst results in similar oxygen radical species. It seems feasible that is the common species, which could be produced from both reactants (O_2 or CO_2) and get stabilized in the oxide ion vacancy site. Based on the above results, it seems likely that a radical reaction mechanism (see below) is responsible for the selective reaction to ethene, but thermal dehydrogenation and cracking also contribute to conversion.

$$\ddot{V}_{O^{2-}} \Leftrightarrow \ddot{V}_{O}^{\cdot -} + h^+$$

$$CO_2 + \ddot{V}_{O}^{\cdot -} \rightarrow CO + O^{\cdot -}$$

$$C_2H_6 + O^{\cdot -} \rightarrow .C_2H_5 + OH^-$$

$$OH^- + h^+ \rightarrow .OH$$

$$.C_2H_5 + .OH \rightarrow C_2H_4 + H_2O$$

or

$$H_2O + \ddot{V}_{O}^{\cdot -} \rightarrow H_2 + O^{\cdot -}$$

In the above mechanism, h^+ indicates a hole, $\ddot{V}_{O}^{\cdot -}$ and $\ddot{V}_{O^{2-}}$ indicate the presence of one electron and no electron in the oxide ion vacancy sites, respectively.

Activation of ethane and propane with $O^{\cdot -}$ was proposed in earlier studies leading the unsaturated analogs [33, 34]. Formation of oxygen radical species from the dissociation of CO_2 is proposed in this work. However, as long as the relevant oxygen species are not properly identified and their role is not elucidated, the reaction mechanism proposed above remains speculation.

4 Conclusions

$Th_{1-x}Ca_xO_2$ solid solution catalysts were synthesized using the solution combustion method and the presence of oxide ion vacancies was indicated by Raman spectroscopy. The catalysts were applied for the oxidative dehydrogenation of ethane with CO_2 in the temperature range 600–750 °C and afforded 97% selectivity to ethene at 46% ethane conversion. Ca-doping of ThO_2 strongly improved the ethene yield. Based on the results of experimental runs without catalyst and in the presence and absence of CO_2 as well as preliminary EPR results we propose that the oxidative dehydrogenation occurs via both thermal dehydrogenation as well as a more selective radical pathway. The latter process seems to be dominant over $Th_{0.75}Ca_{0.25}O_2$ under the applied conditions.

Acknowledgments Financial support by ETH Zurich (TH-09 06-2) is kindly acknowledged. We thank Dr. Maxim Yulikov and Prof. Dr.

Gunnar Jeschke (both ETH Zurich) for providing the EPR measurements and fruitful discussions.

References

1. Cavani F, Koutyrev M, Trifiro F (1996) Catal Today 28:319
2. Kung HH (1994) Adv Catal 40:1
3. Mamedov EA, Corberan VC (1995) Appl Catal A Gen 127:1
4. Blasco T, Nieto JML (1997) Appl Catal A Gen 157:117
5. Banares MA (1999) Catal Today 51:399
6. Heracleous E, Machli M, Lemonidou AA, Vasalos IA (2005) J Mol Catal A 232:29
7. Botella P, Dejoz A, Nieto JML, Concepcion P, Vazquez MI (2006) Appl Catal A Gen 298:16
8. Haddad N, Bordes-Richard E, Barama A (2009) Catal Today 142:215
9. Au CT, Chen KD, Dai HX, Liu YW, Luo JZ, Ng CF (1998) J Catal 179:300
10. Courtine P, Bordes E (1997) Appl Catal A Gen 157:45
11. Routray K, Reddy KRSK, Deo G (2004) Appl Catal A Gen 265:103
12. Ward MB, Lin MJ, Lunsford JH (1977) J Catal 50:306
13. Morales E, Lunsford JH (1989) J Catal 118:255
14. Takahara I, Chang WC, Mimura N, Saito M (1998) Catal Today 45:55
15. Wang S, Murata K, Hayakawa T, Hamakawa S, Suzuki K (2000) Appl Catal A Gen 196:1
16. Zhu J, Qin S, Ren S, Peng X, Tong D, Hu C (2009) Catal Today 148:310
17. Solymosi F, Nemeth R (1999) Catal Lett 62:197
18. Mimura N, Takahara I, Inaba M, Okamoto M, Murata K (2002) Catal Commun 3:257
19. Mimura N, Okamoto M, Yamashita H, Oyama ST, Murata K (2006) J Phys Chem B 110:21764
20. Zhao X, Wang X (2006) Catal Commun 7:633
21. Nakagawa K, Kajita C, Okumura K, Ikenaga N, Nishitani-Gamo M, Ando T, Kobayashi T, Suzuki T (2001) J Catal 203:87
22. Valenzuela RX, Bueno G, Solbes A, Sapina F, Martinez E, Corberan VC (2001) Top Catal 15:181
23. Baidya T, van Vegten N, Jiang Y, Krumeich F, Baiker A (2011) Appl Catal A Gen 391:205
24. Patil KC, Aruna ST, Mimani T (2002) Curr Opin Solid State Mater Sci 6:507
25. Khomane RB, Kulkarni BD, Paraskar A, Sainkar SR (2002) Mater Chem Phys 76:99
26. Jin L, Reutenauer J, Opembe N, Lai M, Martenak DJ, Han S, Suib SL (2009) ChemCatChem 1:441
27. McBride JR, Hass KC, Poindexter BD, Weber WH (1994) J Appl Phys 76:2435
28. Banerji A, Grover V, Sathe V, Deb SK, Tyagi AK (2009) Solid State Commun 149:1689
29. Li SP, Lu JQ, Fang P, Luo MF (2009) J Power Sources 193:93
30. Askrabic S, Dohcevic-Mitrovic ZD, Radovic M, Scepanovic M, Popovic ZV (2009) J Raman Spectrosc 40:650
31. Martinez-Ramireza S, Sanchez-Cortesa S, Garcia-Ramosa JV, Domingoa C, Fortesb C, Blanco-Varelab MT (2003) Cem Conc Res 33:2063
32. Heracleous E, Lemonidou AA (2004) Appl Catal A Gen 269:123
33. Alka K-I, Lunsford JH (1977) J Phys Chem 81:1393
34. Leveles L, Seshan K, Lercher JA, Lefferts L (2003) J Catal 218:307